http://dx.doi.org/10.5607/en.2016.25.3.130
Exp Neurobiol. 2016 Jun;25(3):130-138.
pISSN 1226-2560 • eISSN 2093-8144

Original Article

Experimental Neurobiology

Cerebral Hemodynamics and Vascular Reactivity in Mild and Severe Ischemic Rodent Middle Cerebral Artery Occlusion Stroke Models

Jeongeun Sim[1#], Areum Jo[1#], Bok-Man Kang[2#], Sohee Lee[1#], Oh Young Bang[3,4], Chaejeong Heo[1], Gil-Ja Jhon[5], Youngmi Lee[5] and Minah Suh[1,2,4*]

[1]Center for Neuroscience Imaging Research (CNIR), Institute for Basic Science (IBS), Suwon 16419,
[2]Department of Biomedical Engineering, Sungkyunkwan University, Suwon 16419,
[3]Department of Neurology, Neuroscience Center, Samsung Medical Center, Sungkyunkwan University School of Medicine,
[4]Department of Health Sciences and Technology, SAIHST, Sungkyunkwan University, Seoul 06351,
[5]Department of Chemistry and Nano Science, Ewha Womans University, Seoul 03760, Koera

Ischemia can cause decreased cerebral neurovascular coupling, leading to a failure in the autoregulation of cerebral blood flow. This study aims to investigate the effect of varying degrees of ischemia on cerebral hemodynamic reactivity using *in vivo* real-time optical imaging. We utilized direct cortical stimulation to elicit hyper-excitable neuronal activation, which leads to induced hemodynamic changes in both the normal and middle cerebral artery occlusion (MCAO) ischemic stroke groups. Hemodynamic measurements from optical imaging accurately predict the severity of occlusion in mild and severe MCAO animals. There is neither an increase in cerebral blood volume nor in vessel reactivity in the ipsilateral hemisphere (I.H) of animals with severe MCAO. The pial artery in the contralateral hemisphere (C.H) of the severe MCAO group reacted more slowly than both hemispheres in the normal and mild MCAO groups. In addition, the arterial reactivity of the I.H in the mild MCAO animals was faster than the normal animals. Furthermore, artery reactivity is tightly correlated with histological and behavioral results in the MCAO ischemic group. Thus, *in vivo* optical imaging may offer a simple and useful tool to assess the degree of ischemia and to understand how cerebral hemodynamics and vascular reactivity are affected by ischemia.

Key words: Stroke, MCAO model, Optical intrinsic signal imaging, Hemodynamics, Arterial reactivity

INTRODUCTION

Normal neurovascular coupling between neuronal activity and cerebral blood flow is critical to ensure the health of the brain, and this coupling is vulnerable to ischemic brain diseases. A reduction in cerebral blood flow (CBF) around occluded cerebral vessels leads to a series of biochemical, biomolecular, and functional damage that triggers neuronal cell death pathways [1, 2]. These cascade actions eventually result in disrupted hemodynamic autoregulation and neurovascular coupling malfunctions [3], which are accompanied by ischemia-induced behavioral deficits [4]. Moreover, the severity of ischemia is closely related to sensory

Received April 19, 2016, Revised June 15, 2016,
Accepted June 16, 2016

*To whom correspondence should be addressed.
TEL: 82-31-299-4496, FAX: 82-31-299-4506
e-mail: minahsuh@skku.edu
#These authors contributed equally to this work.

stimulation-induced hemodynamic responses and the functional recovery of sensorimotor functions [5, 6]. In addition, human stroke patients exhibit disruptive neurovascular coupling, which manifests as a reduction in cerebral blood flow [7, 8]. Clinically, it is important to predict infarct regions following ischemia, and there has been an attempt to use reduced hemodynamics, such as CBF, as an early indicator of ischemic stroke.

The middle cerebral artery occlusion (MCAO) model is a common animal model of ischemic stroke. MCAO induces cerebral ischemia and disrupts cerebral autoregulation. However, a dynamic evaluation of the failure in cerebral autoregulation has not yet been undertaken. To compensate for dysfunctional autoregulation, post-ischemic angiogenesis occurs in MCAO [9]. As early as 12 h after ischemia, endothelial cells within the neurovascular coupling unit proliferate from preexisting vessels and make junctional structures in the surrounding infarcted brain tissue [10, 11]. Because hemodynamics in the infarcted brain is affected by this disruption in autoregulation and post-ischemic angiogenesis, it is important to measure hemodynamics in an animal stroke model to evaluate the degree of ischemia. In addition, the degree of ischemia affects functional recovery surrounding the infarction following reperfusion from the ischemic state [12]. The penumbra zone, a functionally impaired but not yet irreversibly injured tissue, is very dynamic and a crucial therapeutic target to improve clinical outcomes. We induced both moderate and severe infarct in MCAO models and measured whether the level of hemodynamic reactivity is dependent on the degree of ischemia.

Cortical electrical stimulation enhances cortical excitability and brings about robust cerebral blood volume (CBV) change, which mimics CBV changes during an epileptic event, which is a most hyper-excitable and hyper-synchronous brain activity [13]. Optical recording of intrinsic signal (ORIS) is one of many functional perfusion-imaging technologies that can be utilized in conjunction with electrical stimulation that does not require injecting special chemicals [14, 15]. ORIS with multi-wavelengths can be used to map neuronal activities derived from the oxygenation states of hemoglobin and changes in CBV [16]. In addition, ORIS with a high-speed, charge-coupled device (CCD) is capable of creating continuous two-dimensional brain surface images, including pial vasculature. Therefore, in the MCAO ischemic models, we utilize ORIS with direct external stimulation to evaluate cortical hemodynamics and vessel reactivity in relation to the degree of ischemia. Our particular interest is whether the MCAO models with different degrees of ischemic severity exhibit differential hemodynamic responses in cerebral arteries and cortical tissue immediately after the application of an external electrical stimulus.

MATERIALS AND METHODS

Animal preparation and MCAO modeling

All animal preparations and procedures were performed in accordance with the Institutional Animal Care and Use Committee (IACUC) of Sungkyunkwan University. Male, 9-week-old, Sprague-Dawley rats (280~320g) were used (OrientBio, Seongnam, South Korea). All rats were housed in humidity- and temperature-controlled facilities with 50~60% humidity at 23°C under a 12-h light/dark cycle.

For the MCAO procedure, the rats were anesthetized and maintained with 2% isoflurane and oxygen gas (VetEquip, CA, USA). A heating pad was used to maintain the animal's body temperature throughout the procedure (FHC, ME, USA). We carefully made an incision in the neck skin and exposed the right common carotid artery (CCA). A 4-0 monofilament nylon suture coated with silicon was introduced from the CCA into the middle cerebral artery (MCA). The insertion length of the suture (18~20 mm) and thickness of the silicon head (330~380 μm) varied according to the body weight of the animal [17]. After MCA occlusion, the incision was temporarily closed and the animal was returned to home cage for either 60 min (N=3) or 90 min (N=12). Then, the animal was anesthetized again with 2% isoflurane, the silicon-coated suture was removed for reperfusion, and the incision was closed.

Behavioral testing using the modified Neurological Severity Score (mNSS)

According to prior studies, the infarct volume of the MCAO model reached a maximum after 24 h of reperfusion [18]. Therefore, we conducted the mNSS behavioral testing after 24 to 72 h of reperfusion. We focused on assessing primary sensory cortical functions to compare the hemodynamic changes in the primary sensory cortex and behavioral consequences in the MCAO model. The mNSS is composed of three different behavioral tests: motor, sensory, and beam balance tests (Fig. 1A). Detailed mNSS procedures were described by Chen et al. (2001) [19].

Optical Recording of Intrinsic Signal (ORIS) imaging

We performed the ORIS imaging right after completion of the behavioral test. We carefully removed the skull of both hemispheres under 2% isoflurane anesthesia. The animal's health was carefully monitored throughout the experiment. Two tungsten electrodes (Plastics One, Roanoke, VA, USA) were placed onto the intact dura mater of each hemisphere (Fig. 1B), which were connected to a pulse generator (Master-8, A.M.P.I., Jerusalem, Israel). Functional hemodynamic imaging was performed using an optical imaging

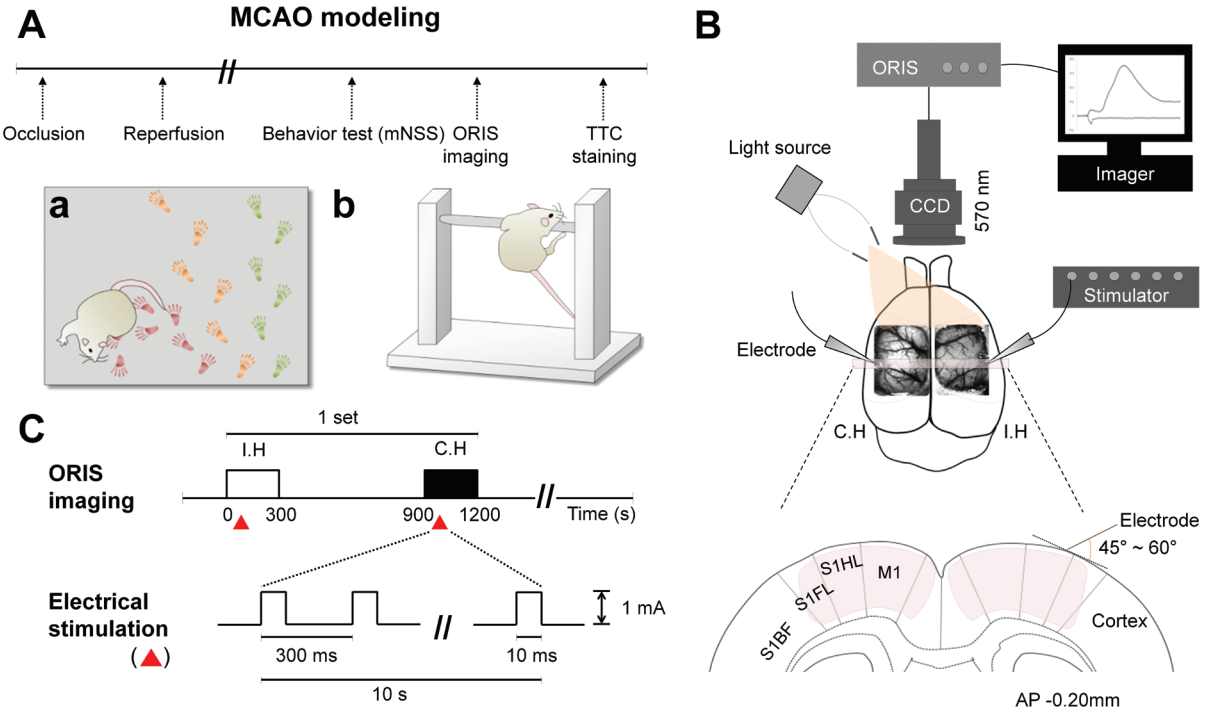

Fig. 1. A diagram of optical recording of intrinsic signal (ORIS) imaging in the MCAO model. (A) The middle cerebral artery occlusion (MCAO) was performed for 60 min or 90 min and then reperfused. Behavior tests such as the walking evaluation (a), the beam balance test (b), and the sensory response test were conducted. (B) Illustration of ORIS imaging. The areas expected to react to the electrical stimulation were denoted as pale-red color (M1, motor cortex; S1HL, hindlimb somatosensory cortex; S1FL, forelimb somatosensory cortex; S1BF, barrel field somatosensory cortex). (C) The experimental scheme depicting ORIS imaging for 300 s and electrical stimulation (red arrow head) for 10 s is shown.

system (Imager 3001, Optical Imaging, Rehovot, Israel) with an external light source (Leica Microsystems, Manheim, Germany). Reflected light was collected through two 50 mm tandem lenses (Nikon, Tokyo, Japan) and filtered using a 570±10 nm band-pass filter. The 570 nm is the isosbestic wavelength of total hemoglobin, which is equivalent to CBV changes. The images were acquired for 300 s at 3.33 Hz. The images recorded during the initial 30 s before applying 10 s stimulation (1 mA, 3.33 Hz, 10 ms pulse width) to the cortex were averaged and designated as the baseline image. Both the ipsilateral hemisphere (I.H), which had the infarction, and the opposite contralateral hemisphere (C.H) were alternatively imaged. In order to ensure hemodynamic recovery to baseline levels, the inter-trial interval was set at 900 s (Fig. 1C).

TTC staining and quantification of infarct volume

After ORIS imaging, the entire brain of the rat was extracted and sectioned into six coronal slices, 2 mm thick, using a rat brain matrix (World Precision Instruments, Sarasota, FL, USA). All coronal slices were stained with 2% 2,3,5-triphenyltetrazolium chloride (TTC) solution (Sigma-Aldrich, St. Louis, MO, USA) for 20 min and fixed with 4% paraformaldehyde at 4°C. After 24 h of initial staining, the six slices were photographed with a graduated ruler using a digital camera (Canon, Tokyo, Japan). The infarct volume of each slice was quantified using Fiji software (NI.H, MD, USA). We classified the MCAO models into two groups according to their infarct volume; the mild MCAO group had less than 90 mm^3 of infarct area that was primarily located in the striatum, while the severe MCAO group had greater than 90 mm^3 of infarct area that included areas in the cortex as well as the striatum.

Image processing for hemodynamic response in the cortical tissue

The activation maps shown in Fig. 3A, C, and E were calculated by dividing every frame by the mean of the baseline frame. We measured the time course of CBV change in the region of interest (ROI, 7×7 pixels) of the cortical tissue, quantifying both the maximum value of CBV change and the time to reach that maximum value. The ROI that was selected included the tissue area that showed the strongest CBV changes but excluded the large vessels. The ORIS data were analyzed using custom-written MATLAB software (MathWorks, Natick, MA, USA).

http://dx.doi.org/10.5607/en.2016.25.3.130

Image processing for hemodynamic reactivity in the pial artery

To compare hemodynamic differences in the arteries between the MCAO and normal groups, we defined the reactive artery from images and quantified them as shown in Fig. 4A. First, the raw images were cropped (3.7×5.9 mm^2) and segmented into cerebral blood vessels and surrounding tissues using the trainable Waikato Environment for Knowledge Analysis (WEKA) segmentation plugin, which combines a collection of machine learning algorithms in Fiji [20]. Based on the segmentation results, the probability of each pixel in the raw image belonging to the segmented vessel was verified by the WEKA tool. The verified pixel probabilities, from 0% to 100%, were mapped in an intensity form. For accurate extraction of the blood vessel without intervention, such as a cerebral hemorrhage and unintended light reflection from the dura mater, we set the threshold value at 60% of the probability for vessel classification (Fig. 4A). This threshold value was a balance between the detection ratio and a false-positive ratio and was determined through an empirical analysis. In a sequence, the reactive region was defined by mapping the standard deviations (SD) of each pixel's value over time. All maps were filtered by a 3×3 Gaussian kernel to prevent the signals from interfering with the outliers. To exclude a low level of variation, which was defined as no response over time, a total of 1,500 pixels were gathered from the highest value in the calculated SD map and were binary coded. A binary coded image was multiplied to all frames of the vessel probability maps in order to extract the reactive vessels, which were defined as arteries, from the vessel probability map (Fig. 4A). The final step of quantification was to measure the time course of CBV change in the extracted artery in each frame. The measured intensity of artery was calculated to extract hemodynamic characteristics, such as maximum ΔCBV and time to peak to compare the differences between the groups using statistical analyses with Kruskal-Wallis nonparametric tests. SD mapping, binary coded images, and statistical analyses were all performed using the custom-written MATLAB software.

RESULTS

Classifications of the mild and severe MCAO models

The MCAO rats were separated into two groups, a mild MCAO group (N=5) and a severe MCAO group (N=10), according to the volume of the infarct (Fig. 2B-D). The majority of the animals that received 90 min of occlusion had severe ischemia, while all of the animals that received 60 min of occlusion and 2 animals that received 90 min of occlusion had mild ischemia. The infarct area in the mild MCAO model was primarily in the striatum (Fig. 2C), while the severe MCAO group exhibited infarcts in both the cortex and subcortical areas (Fig. 2D). Fig. 2A describes the behavioral and physical discrimination between the mild and severe MCAO groups. The average infarct volume of the severe MCAO model (275.44±32.97 mm^3) was significantly greater (p value<0.001) than that of the mild MCAO model (15.69±5.88 mm^3). In the severe MCAO groups, animals had a higher mNSS score (mild MCAO, 6.0±1.05 points; severe MCAO, 9.9±0.35 points; p value<0.001) and greater weight loss than the mild MCAO group (normalized to weight before MCAO; average±SEM; mild MCAO, 95.02±2.50%; severe MCAO, 83.88±1.80%; p value=0.003; independent t-test).

Post-stroke effects on cerebral hemodynamics

In the normal group, CBV around the stimulating electrode increased immediately after the electrical stimulation and peaked in both hemispheres at about 105 s, as shown in two-dimensional images of the whole hemisphere (Fig. 3A, B). In the mild MCAO group, the CBV increase following electrical stimulation was also observed in both hemispheres (Fig. 3C, D). In the severe MCAO

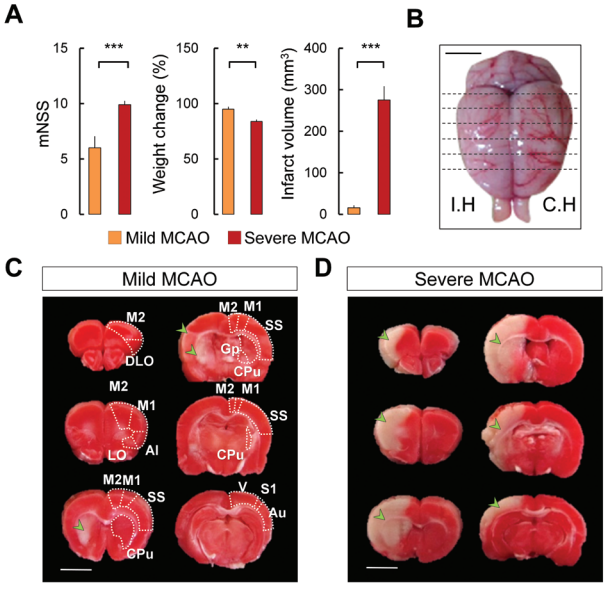

Fig. 2. The pathophysical results from the mild and severe MCAO groups. (A) The average mNSS, weight changes, and infarct volume among the groups are presented (average±SEM; **p value<0.01, ***p value<0.001, independent t-test). (B) Black dashed lines on the brain indicate the positions of 6 coronal sections with 2 mm thickness for TTC staining. (C, D) TTC-stained representative images from the mild MCAO (C) and the severe MCAO (D) models. Green arrows on the brain indicate the infarct (M1, primary motor cortex; M2, secondary motor cortex; SS, somatosensory cortex; S1, primary sensory cortex; Cpu, caudate putamen; Gp, globus pallidus; DLO, dorsolateral orbital cortex; AI, agranular insular cortex; LO, lateral orbital cortex; Au, auditory cortex; V, visual cortex; Scale bar=5 mm).

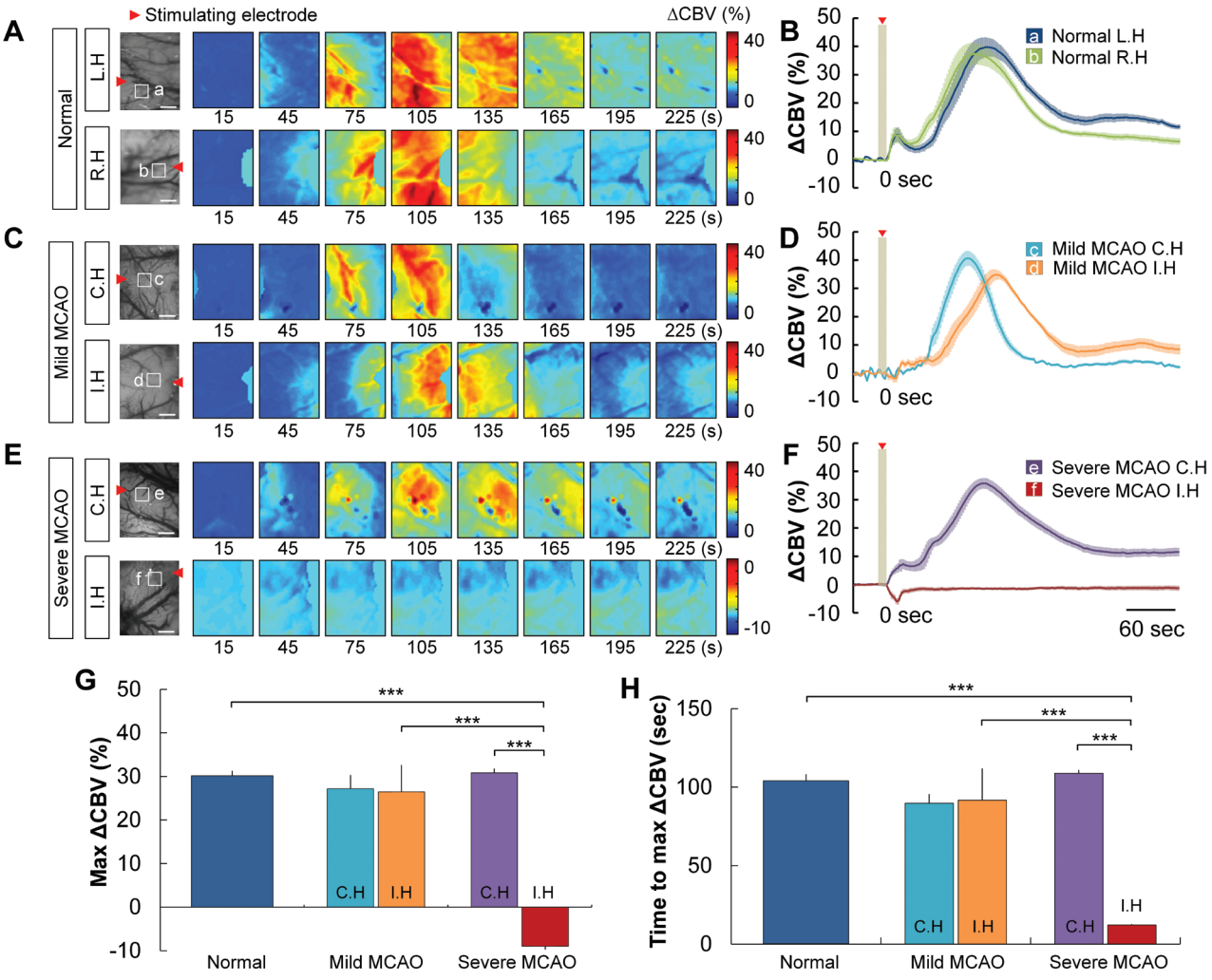

Fig. 3. CBV changes in both hemispheres of the normal mouse and the two MCAO models. (A, C, E) A representative image of the hemodynamic response maps 15 s after the baseline period in the normal (A), mild MCAO (C), and severe MCAO (E) groups. The red arrowhead on the raw cortical image from ORIS indicates the position of the electrode (Scale bar=1 mm). (B, D, F) A time course of the maximum CBV change in the tissue area (a-f; ROI: 7×7 pixels) of the normal, mild MCAO, and severe MCAO groups is shown. The maximum value of the CBV (G) and time to maximum CBV change (H) was calculated in the normal (*N*=10), mild MCAO (*N*=5), and severe MCAO (*N*=10) groups (average±SEM; ***p value<0.001, ANOVA with Bonferroni post-hoc analysis).

group, the CBV of the I.H decreased slightly in the region around the stimulating electrode, while the CBV of the C.H increased after electrical stimulation (Fig. 3E, F).

The maximum CBV change in both hemispheres increased by 30.13±1.16% at 104±4.16 s after stimulation in the normal group. As expected, CBV change in the I.H of the severe MCAO group (-8.98±0.72%) was significantly lower than CBV change in the corresponding C.H (30.83±0.94%) (average±SEM; p value<0.001, paired *t*-test) (Fig. 3G). The I.H of the severe MCAO group showed significant differences in maximum CBV (p value<0.001) and time to reach to maximum peak (p value<0.001) compared to the normal group, while both the maximum CBV change (C.H, 26.45±3.92%; I.H, 27.19±1.98%) and the time to reach the maximum CBV change (C.H, 91.65±12.87 s; I.H, 89.80±3.69 s) in the mild MCAO group showed non-significant differences compared to the normal group (max CBV, p value=0.912; time to max ΔCBV, p value=0.923) (Fig. 3G-H). In the severe MCAO animal, direct electrical stimulation onto the somatosensory cortex created an altered pattern of CBV change in the ipsilateral hemisphere compared with standard CBV changes in that region. Thus, normal autoregulation of neurovascular coupling may be significantly disrupted on the ipsilateral side of severe MCAO animals.

http://dx.doi.org/10.5607/en.2016.25.3.130

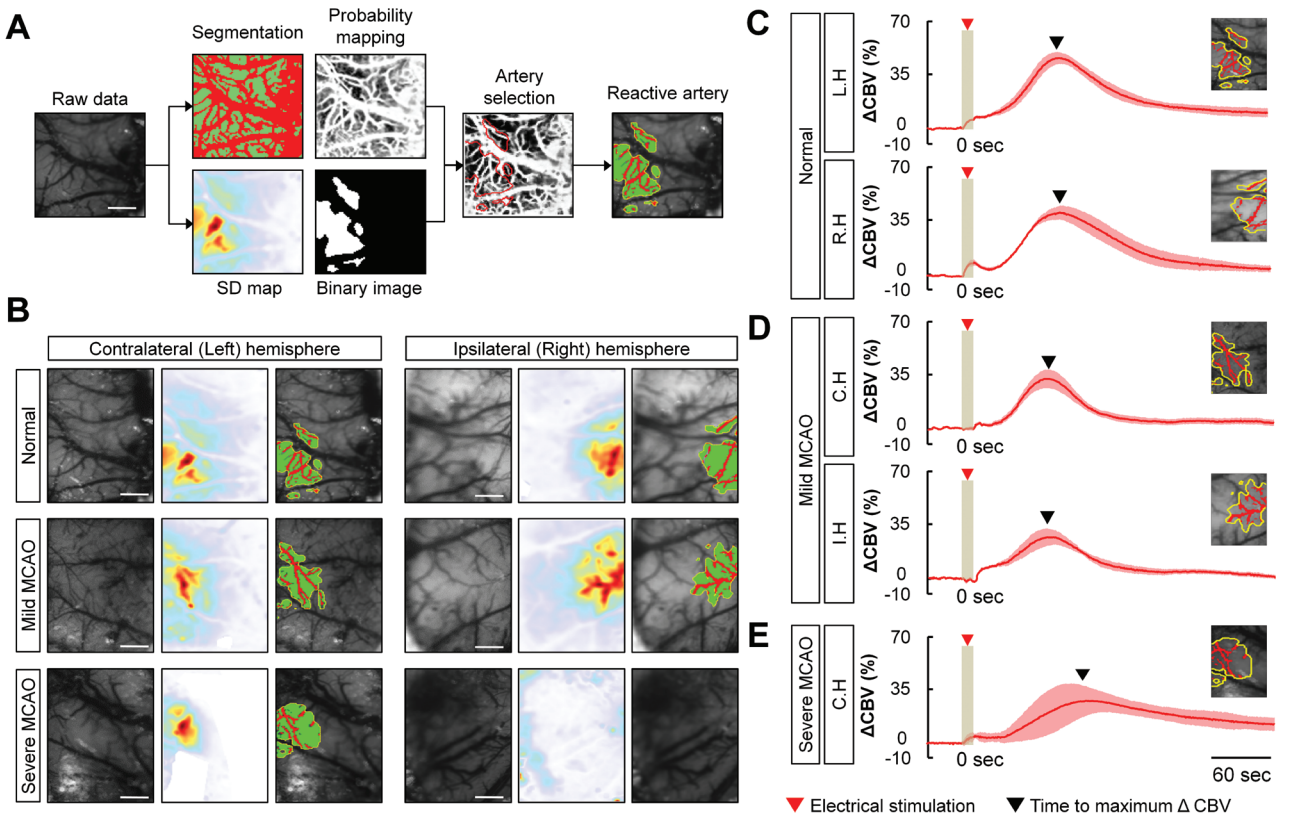

Fig. 4. Reactive cerebral artery extraction using standard deviation (SD) map categorization is shown. (A) Image processing steps for the reactive artery extraction. The artery vasculature was segmented by combining the WEKA segmentation method and SD mapping. Finally, the reactive artery (red) was overlapped on the reactive area (green). (B) Representative vessel segmentation procedures. A raw image (first column), a color-coded SD map (second column), and the segmented vessel within the reactive area (third column) of the normal (first row), mild MCAO (second row), and severe MCAO (third row) groups in both hemispheres are shown (Scale bars=1 mm). (C) Dynamic changes in the reactive artery in the normal brain cortex following a 10-s electrical stimulation (*N*=10). (D) The averaged artery reactivity in the mild MCAO group (*N*=4) and the E: Severe MCAO group (*N*=5) is shown (Error bar, SEM).

Analysis of vascular reactivity in the MCAO models

To examine arterial responsiveness as the increase in CBV spreads throughout the infarcted brain, we segmented arteries using the WEKA methods (Fig. 4A). Representative images of the reactive artery (red color) are shown in Fig. 4B. However, segmented arteries could not be obtained from the I.H of the severe MCAO model because electrical stimulation to the I.H of the severe MCAO group did not cause a significant change in CBV. The averaged maximum change in CBV in arteries increased up to 39.91±1.57% at 93.85±4.87 s in the normal group (Fig. 4C). The CBV change in arteries of the mild MCAO group was faster (C.H, 78.45±7.19 s, p value=0.090; I.H, 53.70±14.10 s, p value=0.005) and smaller (C.H, 31.99±2.60%, p value=0.275; I.H, 26.65±7.38%, p value=0.379) than normal group in both hemispheres during electrical stimulation (Fig. 4D), which was distinct from the hemodynamic reactivity in tissue (Fig. 3G-H). In the C.H of the severe MCAO group, the reaction of the arteries was the slowest (109.45±3.58 s) and the smallest (27.75±2.34%) compared with the C.H of the other groups (Fig. 4E). The differences of the time to reach maximum CBV change of the artery were statistically significant in the C.H of the severe MCAO group compared with the normal (p value=0.023) and C.H in mild MCAO (p value=0.014) groups. However, the maximum CBV change of the tissue area in the C.H of the severe MCAO group was not significantly different among the three groups (Fig. 3G). These results suggest that in the severe MCAO group, the autoregulatory function of arteries in the contralateral hemisphere was disrupted.

Correlation analysis between hemodynamic function and severity of the ischemia

We next investigated whether hemodynamic reactivity was correlated with the severity of ischemia in Fig. 5. We correlated pathophysical indexes (mNSS, weight loss, and infarct size) with the hemodynamic indexes (maximum change in pixel

A

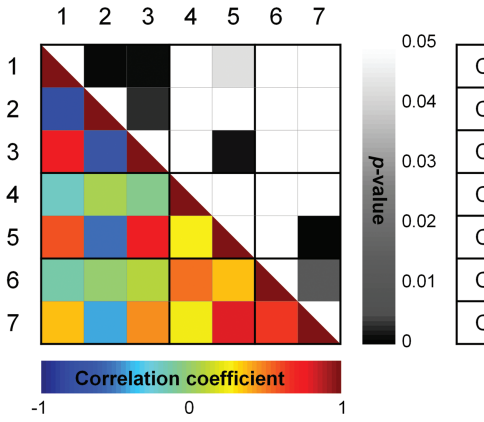

Component 1	Pathophysical index	mNSS
Component 2		Weight change
Component 3		Infarct size
Component 4	Artery index	Maximum Δ CBV
Component 5		Time to peak of Δ CBV
Component 6	Tissue index	Maximum Δ CBV
Component 7		Time to peak of Δ CBV

B

		Tissue index		Artery index	
		Max Δ CBV	Time to peak	Max Δ CBV	Time to peak
mNSS	Correlation coefficient	-0.140	0.371	-0.098	0.567
	p-value	0.649	0.212	0.751	0.043 *
Weight change	Correlation coefficient	-0.022	-0.426	0.079	-0.534
	p-value	0.942	0.147	0.798	0.060
Infarct size	Correlation coefficient	0.091	0.462	0.158	0.738
	p-value	0.767	0.112	0.605	0.004 **

**. Correlation is significant at the 0.01 level (2-tailed).
*. Correlation is significant at the 0.05 level (2-tailed).

Fig. 5. The correlation coefficient matrix showing the relationships between the pathophysical indexes and hemodynamic indexes in segmented artery and tissue area. (A) The lower left triangle with the color scale indicates a correlation coefficient between indexes, while the upper right triangle with the gray scale indicates the significance of the correlation coefficients. Pearson's correlation analysis was used, and the gray scale only displays statistically significant p-values. (B) Summary of correlation coefficient and p-value (*, Correlation is significant at the 0.05 level; **, Correlation is significant at the 0.01 level).

intensity and time to maximum pixel intensity) of segmented artery and tissue ROI. The time to peak ΔCBV in artery has the highest correlation score with infarct size among all correlations (r=0.738, p value=0.004) (Fig. 5A). Fig. 5B summarizes correlation coefficient values from correlation analysis of quantified hemodynamic values of the three groups along with pathophysical information.

DISCUSSION

The main purpose of our study was to explore the effect of cerebral ischemia on cerebral hemodynamics and the reactivity of the pial artery by employing *in vivo* ORIS imaging. In particular, we investigated the hemodynamic patterns of pial artery response after direct cortical stimulation in both normal and penumbra-like areas of ischemic brains. Additional interest is the degree of correlation among (1) our measured hemodynamic responses from the neuronal activation induced by electrical stimulation, (2) standard neurological testing for the MCAO model, and (3) pathophysical results. ORIS imaging was utilized because it has good spatio-temporal resolution for *in vivo* brain imaging and is easy to implement. ORIS imaging is also economically efficient in real-time monitoring of hemodynamic responses including vessel reactivity over the cortical surface of the whole brain.

MCAO is an effective method to induce ischemic damage in rodent brains. With this technique, reperfusion can be easily achieved, and the duration of occlusion can be varied; thus, the degree of ischemia is effectively controlled in the MCAO model [17, 21]. The gold standard to assess the effect of MCAO in rodent models is to measure neuro-behavioral scores as well as the infarct size using histopathological procedures after death [19]. For more direct monitoring, numerous neuroimaging studies have been conducted that measured hemodynamic responses following MCAO including methodologies such as magnetic resonance

http://dx.doi.org/10.5607/en.2016.25.3.130

imaging [22], positron emission tomography [23], and laser-Doppler flowmetry [24].

Our study differs from previous investigations because we assessed the severity of the MCAO and performed comparative vascular reactivity and functional hemodynamic studies based on *in vivo* ORIS imaging. With ORIS, it is quite easy to acquire a brain surface image with clear vasculature in the MCAO animal and simultaneously record functional hemodynamic changes. Arteries have smooth muscle to control the supply of blood flow by dilating and contracting, and therefore, it is known that arteries are the most reactive during neurovascular coupling. Particularly, the dilation capacity of arteries is an important index to evaluate hemodynamic functionality *in vivo* [25, 26]. Therefore, we focused on characterizing the reactivity of arteries in both the severe and mild MCAO groups. Reactivity and reaction time of the cerebral arteries should vary with the severity of infarction. By utilizing ORIS image analyses in normal and MCAO animals, we quantified the variation and the reaction of the arteries to electrical stimulation. Our SD analyses of vascular images confirmed that the major component of vascular reactivity during electrical stimulation stems from artery dilations. In our study, the mild MCAO group, which had little striatal infarct, showed an interesting pial arterial reactivity. In response to the neuronal activity induced by direct electrical stimulation, the mild MCAO group had sharply changing vessel reactivity dynamics (Fig. 4D). Many human studies reported that the penumbra area showed mismatch of CBF and CBV owing to direct autoregulatory function to compensate decreased perfusion pressure, whereas infarct core area showed decrease of both CBF and CBV [27-28]. In our results, the reactivity pattern in the I.H of the mild MCAO animals may represent altered hemodynamic functionality of the penumbra surrounding the ischemic infarction.

A dramatic hemodynamic feature of the severe MCAO animal is a decrease of CBV in the I.H following direct cortical electrical stimulation, which can induce strong neuronal activation. In the severe MCAO group, direct electrical stimulation induced neither increases in CBV nor dilations of the arteries on the I.H of the cortex. The degree of deduction greatly depends upon the level of ischemic severity in the MCAO group. Usually, direct cortical electrical stimulation causes an immediate CBV change in the stimulated brain hemispheres, as shown in Fig. 3. However, within the severe MCAO group, the hemisphere with the cortical infarct responded very little to direct cortical electric stimulation; if there was a response, the hemisphere exhibited a decrease in CBV. Perhaps the lack of response results from tissue failure, due to cellular losses such as the astrocytes and pericytes needed for neurovascular coupling, and from dysfunctional angiogenesis. Also, the decreased artery reactivity in the C.H of the severe MCAO group might be due to a broad infarction area in the cortex and, thus, reflects the severity of ischemia.

Overall, the hemodynamic measurements of pial artery responses in the MCAO groups are best correlated with infarct size and neurological severity scores. Therefore, *in vivo* ORIS imaging can be used to predict the degree of infarct following brain ischemia. In this study, we confirmed that the severity of cerebral ischemia is responsible for varying degrees of functional change in cerebral hemodynamics and vessel reactivity. In addition, this study provides insights toward a better understanding of cerebral hemodynamics and vessel reactivity in penumbra-like ischemic tissue.

ACKNOWLEDGEMENTS

This work was supported by the Institute for Basic Science (IBS-R015-D1) in South Korea and the Converging Research Center Program, which is funded by the Ministry of Education, Science and Technology (2013K000267), as well as a grant from the Korean Health Technology R&D Project, Ministry of Health & Welfare, Republic of Korea (A110097).

REFERENCES

1. Barr TL, Conley Y, Ding J, Dillman A, Warach S, Singleton A, Matarin M (2010) Genomic biomarkers and cellular pathways of ischemic stroke by RNA gene expression profiling. Neurology 75:1009-1014.
2. Girouard H, Iadecola C (2006) Neurovascular coupling in the normal brain and in hypertension, stroke, and Alzheimer disease. J Appl Physiol (1985) 100:328-335.
3. Salinet AS, Robinson TG, Panerai RB (2015) Effects of cerebral ischemia on human neurovascular coupling, CO2 reactivity, and dynamic cerebral autoregulation. J Appl Physiol (1985) 118:170-177.
4. Hartman RE, Lee JM, Zipfel GJ, Wozniak DF (2005) Characterizing learning deficits and hippocampal neuron loss following transient global cerebral ischemia in rats. Brain Res 1043:48-56.
5. Bauer AQ, Kraft AW, Wright PW, Snyder AZ, Lee JM, Culver JP (2014) Optical imaging of disrupted functional connectivity following ischemic stroke in mice. Neuroimage 99:388-401.
6. van Meer MP, Otte WM, van der Marel K, Nijboer CH, Kavelaars A, van der Sprenkel JW, Viergever MA, Dijkhuizen RM (2012) Extent of bilateral neuronal network reorganization

and functional recovery in relation to stroke severity. J Neurosci 32:4495-4507.
7. Calautti C, Baron JC (2003) Functional neuroimaging studies of motor recovery after stroke in adults: a review. Stroke 34:1553-1566.
8. Campbell BC, Christensen S, Levi CR, Desmond PM, Donnan GA, Davis SM, Parsons MW (2012) Comparison of computed tomography perfusion and magnetic resonance imaging perfusion-diffusion mismatch in ischemic stroke. Stroke 43:2648-2653.
9. Thored P, Wood J, Arvidsson A, Cammenga J, Kokaia Z, Lindvall O (2007) Long-term neuroblast migration along blood vessels in an area with transient angiogenesis and increased vascularization after stroke. Stroke 38:3032-3039.
10. Hayashi T, Noshita N, Sugawara T, Chan PH (2003) Temporal profile of angiogenesis and expression of related genes in the brain after ischemia. J Cereb Blood Flow Metab 23:166-180.
11. Silvestre JS, Smadja DM, Lévy BI (2013) Postischemic revascularization: from cellular and molecular mechanisms to clinical applications. Physiol Rev 93:1743-1802.
12. Bandera E, Botteri M, Minelli C, Sutton A, Abrams KR, Latronico N (2006) Cerebral blood flow threshold of ischemic penumbra and infarct core in acute ischemic stroke: a systematic review. Stroke 37:1334-1339.
13. Lee S, Koh D, Jo A, Lim HY, Jung YJ, Kim CK, Seo Y, Im CH, Kim BM, Suh M (2012) Depth-dependent cerebral hemodynamic responses following direct cortical electrical stimulation (DCES) revealed by in vivo dual-optical imaging techniques. Opt Express 20:6932-6943.
14. Bartfeld E, Grinvald A (1992) Relationships between orientation-preference pinwheels, cytochrome oxidase blobs, and ocular-dominance columns in primate striate cortex. Proc Natl Acad Sci U S A 89:11905-11909.
15. Sheth SA, Nemoto M, Guiou MW, Walker MA, Toga AW (2005) Spatiotemporal evolution of functional hemodynamic changes and their relationship to neuronal activity. J Cereb Blood Flow Metab 25:830-841.
16. Suh M, Bahar S, Mehta AD, Schwartz TH (2006) Blood volume and hemoglobin oxygenation response following electrical stimulation of human cortex. Neuroimage 31:66-75.
17. Kim DH, Seo YK, Thambi T, Moon GJ, Son JP, Li G, Park JH, Lee JH, Kim HH, Lee DS, Bang OY (2015) Enhancing neurogenesis and angiogenesis with target delivery of stromal cell derived factor-1alpha using a dual ionic pH-sensitive copolymer. Biomaterials 61:115-125.
18. Liu F, Schafer DP, McCullough LD (2009) TTC, fluoro-Jade B and NeuN staining confirm evolving phases of infarction induced by middle cerebral artery occlusion. J Neurosci Methods 179:1-8.
19. Chen J, Li Y, Wang L, Zhang Z, Lu D, Lu M, Chopp M (2001) Therapeutic benefit of intravenous administration of bone marrow stromal cells after cerebral ischemia in rats. Stroke 32:1005-1011.
20. Hall M, Frank E, Holmes G, Pfahringer B, Reutemann P, Witten IH (2009) The WEKA data mining software: an update. SIGKDD Explor 11:10-18.
21. Lee HJ, Park J, Yoon OJ, Kim HW, Lee DY, Kim DH, Lee WB, Lee NE, Bonventre JV, Kim SS (2011) Amine-modified single-walled carbon nanotubes protect neurons from injury in a rat stroke model. Nat Nanotechnol 6:121-125.
22. Bihel E, Pro-Sistiaga P, Letourneur A, Toutain J, Saulnier R, Insausti R, Bernaudin M, Roussel S, Touzani O (2010) Permanent or transient chronic ischemic stroke in the non-human primate: behavioral, neuroimaging, histological, and immunohistochemical investigations. J Cereb Blood Flow Metab 30:273-285.
23. Kobayashi M, Mori T, Kiyono Y, Tiwari VN, Maruyama R, Kawai K, Okazawa H (2012) Cerebral oxygen metabolism of rats using injectable (15)O-oxygen with a steady-state method. J Cereb Blood Flow Metab 32:33-40.
24. Harada H, Wang Y, Mishima Y, Uehara N, Makaya T, Kano T (2005) A novel method of detecting rCBF with laser-Doppler flowmetry without cranial window through the skull for a MCAO rat model. Brain Res Brain Res Protoc 14:165-170.
25. Chen BR, Kozberg MG, Bouchard MB, Shaik MA, Hillman EM (2014) A critical role for the vascular endothelium in functional neurovascular coupling in the brain. J Am Heart Assoc 3:e000787.
26. Takano T, Tian GF, Peng W, Lou N, Libionka W, Han X, Nedergaard M (2006) Astrocyte-mediated control of cerebral blood flow. Nat Neurosci 9:260-267.
27. Murphy BD, Fox AJ, Lee DH, Sahlas DJ, Black SE, Hogan MJ, Coutts SB, Demchuk AM, Goyal M, Aviv RI, Symons S, Gulka IB, Beletsky V, Pelz D, Hachinski V, Chan R, Lee TY (2006) Identification of penumbra and infarct in acute ischemic stroke using computed tomography perfusion-derived blood flow and blood volume measurements. Stroke 37:1771-1777.
28. Sobesky J, Zaro Weber O, Lehnhardt FG, Hesselmann V, Neveling M, Jacobs A, Heiss WD (2005) Does the mismatch match the penumbra? Magnetic resonance imaging and positron emission tomography in early ischemic stroke. Stroke 36:980-985.

 http://dx.doi.org/10.5607/en.2016.25.3.130